

PROTECTING VISIBILITY
AN EPA REPORT TO CONGRESS

CHAPTER 2

2 FUNDAMENTALS OF ATMOSPHERIC VISIBILITY IMPAIRMENT

“Therefore, O Painter, make your smaller figures merely indicated and not highly finished, otherwise you will produce effects opposite to nature, your supreme guide. The object is small by reason of the great distance between it and the eye; this great distance is filled with air, that mass of air forms a dense body which intervenes and prevents the eye from seeing the minute details of the objects.” –Leonardo da Vinci, Six Books on Light and Shade.

2.1 INTRODUCTION: VISION IN THE ATMOSPHERE

Our ability to define, monitor, model and control anthropogenic visibility impairment is dependent on understanding of the scientific and technical factors that affect atmospheric visibility. Visibility involves an observer’s perception of the physical environment. The fundamental factors that determine visibility are illustrated in Figure 2-1 and include:

1. Illumination of the scene by the sun, as mediated by clouds, ground reflection, and the atmosphere;
2. Reflection, absorption, and scattering of incoming light by the target objects and sky resulting in inherent contrast and color patterns at the target location;
3. Scattering and absorption of light from the target and illumination source by the atmosphere and its contaminants;
4. Psychophysical response of the human eye-brain system to the resulting light distribution, and
5. Subjective judgment of the perceived images by the observer.

Evaluation of the effects of air pollution on visibility thus involves two steps: 1) specification of the process of human visual perception and 2) quantification of the impacts of air pollution on the optical characteristics of the atmosphere. The characteristics of illumination and targets can be important to both steps.

2.2 HUMAN VISUAL PERCEPTION

2.2.1 Brightness and Contrast

The eye receives image-forming radiation from the environment and converts it into electrical impulses, which are further interpreted and perceived by the brain. The perception of brightness, contrast, and color is not determined simply by the pattern and

intensity of incoming radiation; rather, it is a dynamic searching for the best interpretation of the available data (Gregory, 1978).

A candle in a brightly lit room is scarcely noticeable; but, if the room is dim to start with, the candle itself appears bright. Similarly, sunlit treetops may appear dark against the horizon sky but bright when viewed against the shadowed forest floor. These examples show that the absolute intensity of radiation has little to do with or brightness perception of visible objects. The eye normally senses and intensity difference *relative* to the overall intensity level; that is, it detects the contrast. Thus, trees that appear darker than background cliffs in bright sunlight will also appear darker than the cliffs in moonlight or heavy overcast.

The detection of contrast between an object and its surroundings is fundamental to visibility. Without contrast, as for example in a thick fog, objects cannot be perceived. As the contrast between object and background is reduced (for example, by increased pollution), the object becomes less distinct. When the contrast becomes very small, the object will no longer be visible. This liminal or *threshold contrast* has been the object of considerable study. The threshold contrast is of particular interest for atmospheric visibility, since it influences the maximum distances at which various components of a scene can be discerned. Of equivalent importance to threshold contrast is the smallest perceptible change in contrast of a viewed scene caused by a small increment in pollution haze.

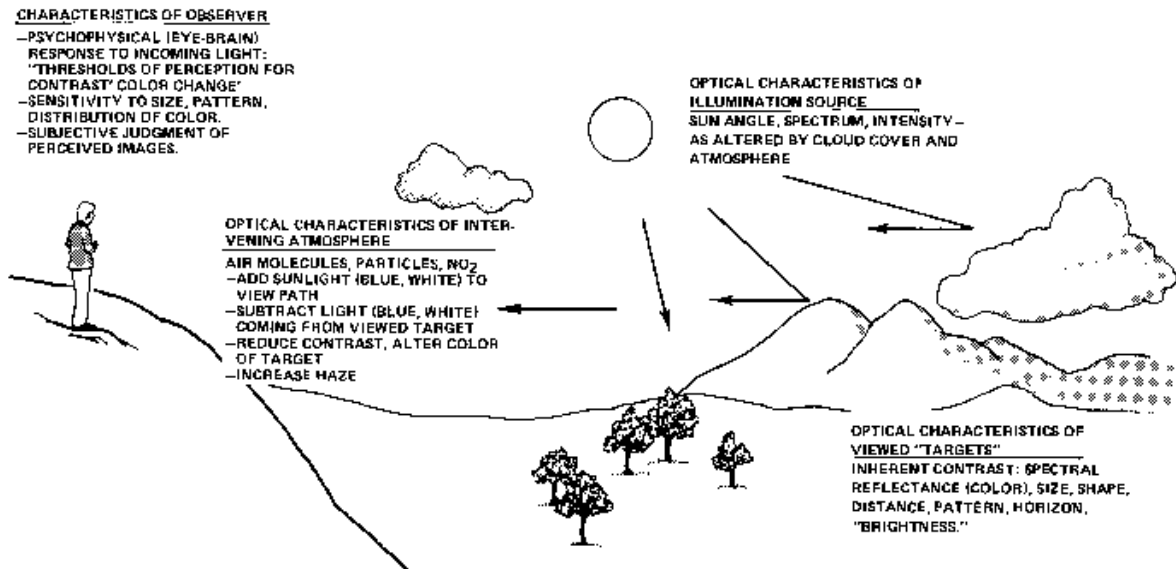


Figure 2-1. Vision in the atmosphere.

The physiology of threshold contrast detection is illustrated in Figure 2-2, showing a bright horizon ($I + \Delta I$) against which a "hazy" mountain (I) is being detected. Laboratory experiments indicate that for most daylight viewing intensities, contrasts ($\Delta I / I + \Delta I$) as low as .018 to .03 (1.8 to 3 %) are perceptible (Figure 2-3).

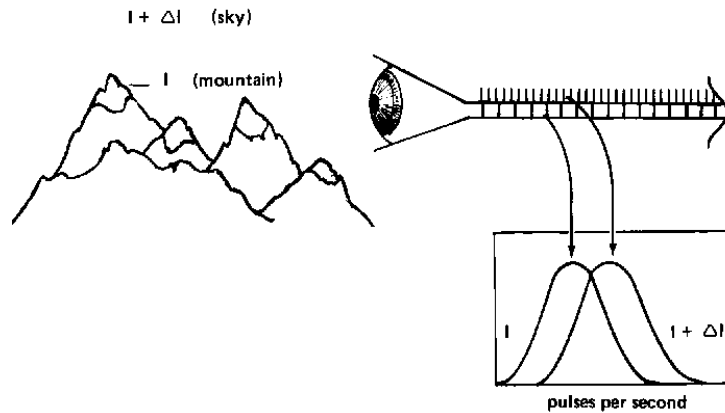


Figure 2-2. Physiological response of the eye to an increment in light intensity is an increase in the number of signals sent to the brain. The detection of threshold contrast involves discrimination of the signal field (I) from its brighter background ($I + \Delta I$) (Gregory, 1978).

Middleton's measurements of observer threshold contrasts for viewing large, dark distant objects in the atmosphere produced similar results, although some variability in observer sensitivity was noted (Figure 2-4). This study, however, was conducted in a relatively polluted urban area. Similar experiments to evaluate contrast thresholds in pristine areas are needed.

The preceding discussion of thresholds was limited to contrast between objects and backgrounds of relatively large apparent size. For "smaller" objects, however, the size of the visual image on the retina of the eye also plays an important role in the perception of contrast. We all know from experience that, as an object recedes from us and apparently becomes smaller, details with low contrast become difficult to perceive. The reason for this loss of contrast perception is not only that the relative brightness of adjacent areas changes but also that the visual system is less sensitive to contrast when the spacing of contrasting areas decreases. If the contrast spacing is regular, a "spatial frequency" can be readily determined. The human visual system is much more sensitive to contrast at certain spatial frequencies than to contrast of other spatial frequencies.

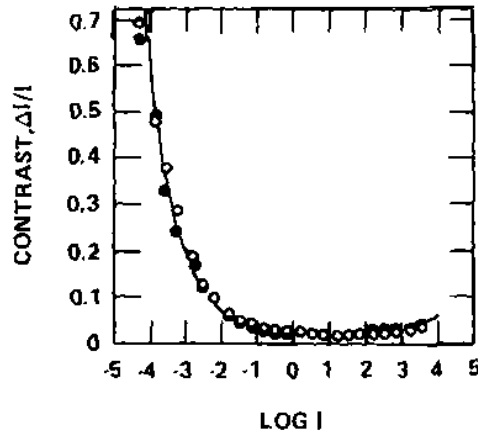


Figure 2-3. The minimum perceptible (threshold contrast $\Delta I/I$ is between .018 and .03 for about four orders of intensity change. Evidently, at low intensities, the statistical 'noise' of retinal signals becomes important; at very high intensities, blinding deteriorates the contrast sensitivity ((Konig and Brodhum, 1889).

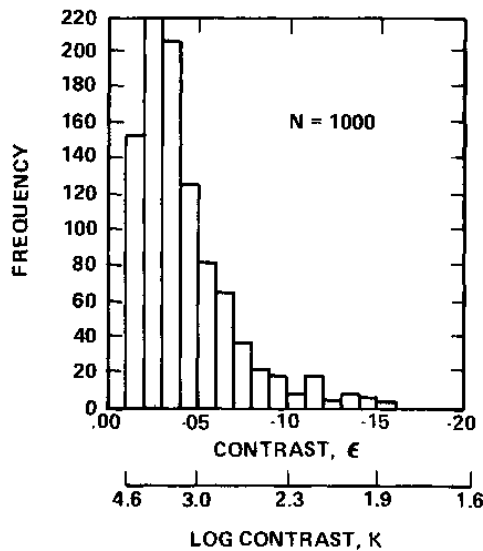


Figure 2-4. Measured threshold contrast of large, dark targets identified in 1000 determinations of visual range by 10 observers. Variability is due to both differences in observer thresholds and the discrete nature of the marker set (Middleton, 1952).

Figure 2-5 shows the contrast sensitivity (inverse of contrast threshold) of the eye-brain system to a standard test pattern with varying spatial frequency. Although several factors affect the location of the curve, the contrast sensitivity is generally highest for periodic visual patterns if the spacings are about 0.33 degrees (20 minutes) apart. This corresponds to clumps of vegetation viewed at a distance of 10 km. The figure indicates that as the visual targets become smaller and their spacing increases, the threshold contrast steadily increases. Measurements of the perceived threshold contrast for individual circular targets suggest a similar relationship (Taylor, 1964). The threshold contrast increases for single targets occupying less than 0.5 degrees (30 minutes) of arc

but remains constant (at about 0.3%) for larger targets. The moon and sun occupy about 30 minutes of arc.

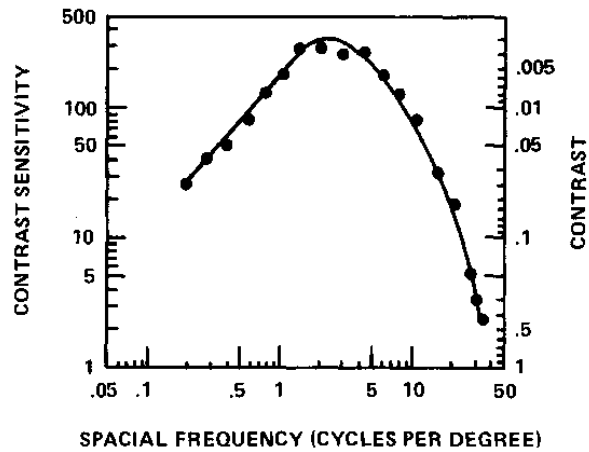


Figure 2-5. Contrast sensitivity of human subjects for sine-wave grating peaks at three cycles per degree corresponding to a contrast threshold of 0.003 or 0.3% (Campbell and Maffei, 1974).

The relationship between perceived contrast threshold and target characteristics (size and pattern) is important for visibility, because a scenic vista usually contains a number of targets of varying sizes and arrangements. The calculation of the perceptibility of all targets would require specification of their angular size distribution. The perception of “texture,” consisting of contours of small angular size and high spatial frequency, is particularly affected by this loss of threshold sensitivity. Henry (1977, 1979) has proposed a system for quantifying this effect through the transformation of the contrast details of a scene in conjunction with a specification of the human psychophysical contrast response function (Figure 2-5). This approach, termed MTF*, has some limitations but theoretically could be used to predict the contrast reduction that would cause a just-noticeable (perceptible) difference in the scene.

Although the MTF approach may ultimately improve the specification of perceptible changes invisibility of contrast detail, it has not yet been fully developed or experimentally tested for atmospheric vision. Thus, current visibility models and assessment tools must rely on evaluation of contrast changes for large dark targets as an index of visual degradation. Even for this kind of target, additional experimental verification of perceptible contrast changes is needed. For the purpose of this report the threshold contrast for large dark targets will be assumed to be 0.02. The minimum perceptible contrast change for large targets is less well quantifies and may vary with initial conditions.. Based on preliminary, unpublished data, the minimum perceptible change may range between 0.01 and 0.05 (Malm, 1979b).

2.2.2 Color

The preceding section discussed the response of the eye and brain to the intensity of light, ignoring the spectral (wavelength) distribution. Color is the sensation produced by the eye-brain system in response to incoming light.

The eye has three different types of color sensors (cones) which cover the visible spectrum in three broad, overlapping curves (Figure 2-6). The system operates so that an object that reflects half blue light and half yellow light is identified not as yellow-blue, but rather as a new color, white. As in the case with brightness, the perception of color is not dependent on the absolute flux of radiant energy reaching the eye. The color of objects (e.g. flesh tones) appears similar over a wide range of outdoor and indoor illumination. The eye differs in this regard from photographic film, which can take on a reddish or bluish cast under differing lighting conditions. Moreover, the color of the surrounding scenery can affect the perceived color of a given object. The normalization of color and other aspects of color perception are not fully understood. Although recent approaches to explaining the mechanism of color perception appear promising (Land, 1977), no completely adequate theory of color vision exists (Henry, 1979).

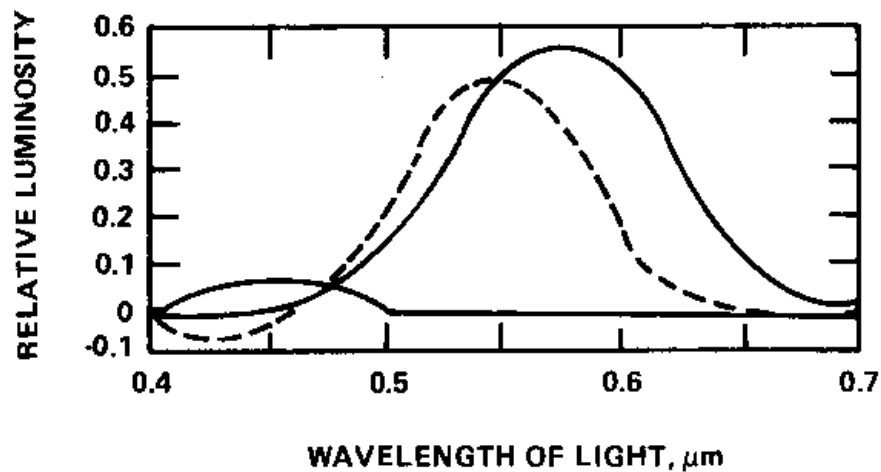


Figure 2-6. The fundamental response curves of the eye (cones). The visible spectrum extends from 0.4 (roughly violet or blue) to 0.7 (roughly red) micrometers. The weighted peak (photopic) response of the eye occurs at a wavelength of 0.55 μm (Gregory, 1978).

The chromaticity diagram (Figure 2-7) was developed to quantify empirically the concept of color. Any three colors, no one of which can be matched by the other two, determine an unambiguous system of coordinates for all colors that can be matched by mixtures of the three; one has only to specify the proportions in the (unique) match. The Commission International de l’Eclairage (CIE) has established two standard schemes, based on three imaginary non-physical colors, by which schemes all colors can be represented as such matches. The CIE primaries, denoted X, Y, Z, are defined in terms of the small field and large field color matching behaviors of a hypothetical “standard observer,” whose response to radiation of various wavelengths is near the average of a number of actual observers with normal color perception. This system allows for complete specification of color through its chromaticity coordinates (x, y) and intensity (L*).

The CIE color metrics enjoy wide use in science and industry as international standards. They must not be thought of as methods for describing sensations or a theory of vision but only as means of assigning numbers to colors in such a way that two colors

that have the same numerical specifications will appear alike to the standard observer under standard viewing conditions.

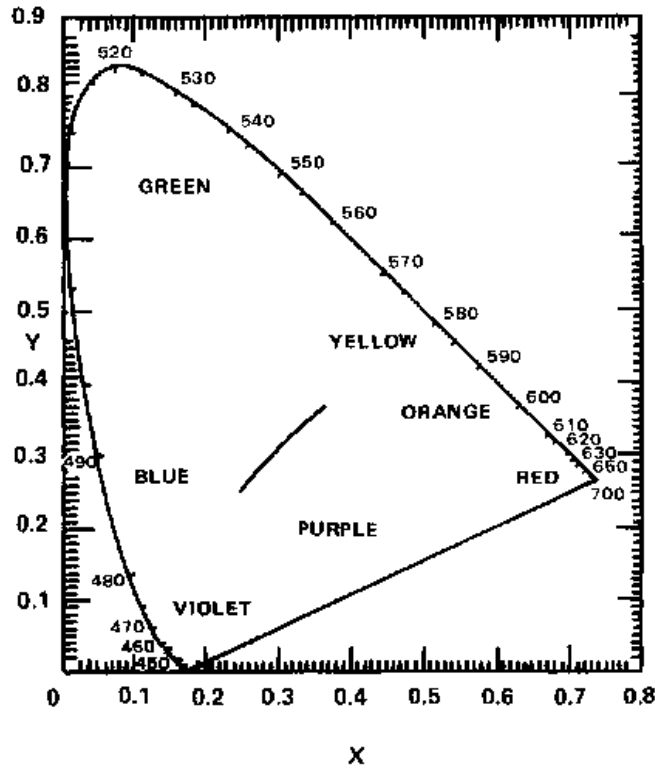


Figure 2-7. The small-field (2°) CIE chromaticity diagram. The curved line is the locus of the spectral colors; all physically realizable colors lie within the closed figure formed by the spectrum locus and the straight line joining its ends. Heavy curve in the middle indicates typical chromaticities of daylight. Intensity or brightness can be represented by a third dimension, perpendicular to the plane of the paper. The corresponding large-field (10°) diagram is similar (adapted from Middleton, 1952).

An attractive feature of the CIE color metrics is that colors that are similar in appearance lie close together on the chromaticity diagrams. A great deal of experimental work has been done on color discrimination thresholds, which are of critical importance to the paint and dye related industries. On the chromaticity diagrams, these thresholds take the form of small ellipses of colors just distinguishable from a given color (Figure 2-8). The differences in colors are specified by a parameter ΔE , which is a function of the change in light intensity or brightness (ΔL^*) and the change in chromaticity ($\Delta x, \Delta y$), ΔE can be considered as a distance between two colors in a color “space” such that equal distances (ΔE) between any two colors correspond to equally perceived color changes. It is possible that a threshold, ΔE_0 , can be found to determine whether a given color change is perceptible. Latimer et al. (1978) have calculated threshold values of ΔE for visible plumes, but the applicability of this system for quantifying perceptible atmospheric discoloration has not yet been experimentally verified.

Factors other than that specified by ΔE (wavelength, intensity) that are of importance to perception include: size of object or area, color of surrounding background, and temporal variations. The well-known effect of background color on perceived color is called chromatic adaptation. In general, if the eye is adapted to a color, e.g. blue sky, a nearby white area may take on the complementary color of the background, in this case a light yellow-brown. This effect may be large enough to explain some of the brown color of atmospheric haze (Henry, 1979).

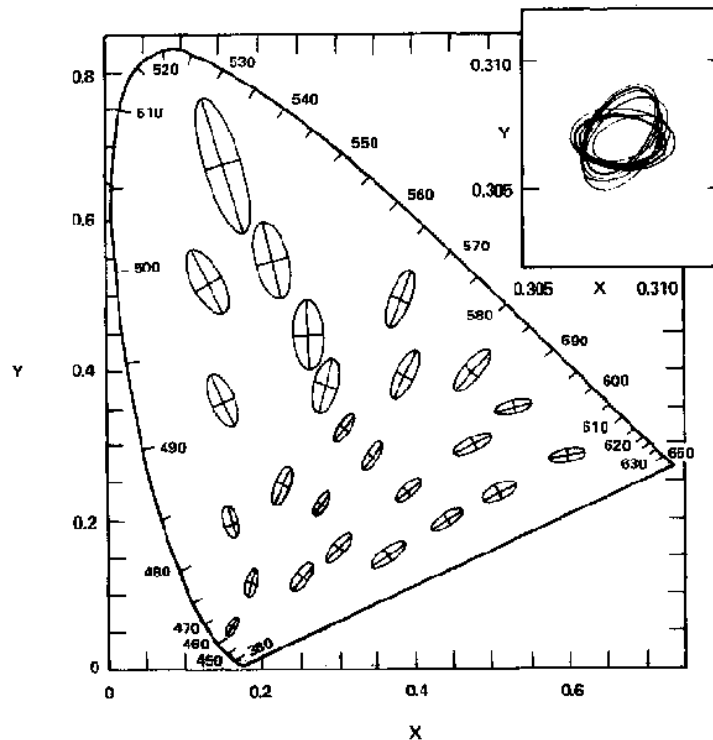


Figure 2-8. Small-field chromaticity diagram showing color-matching ellipses, represented 10 times actual scale for clarity. Each ellipse is the locus of standard deviation in repeated small-field color matching. The diagram summarizes almost 25,000 attempted color matches by a single observer (MacAdam, 1942). Insert: Variability of large-field color-matching ellipsoids among 12 different observers (Brown, 1957).

Because current understanding of color perception is inadequate, theoretical calculations of atmospheric discoloration are useful only as a guide for experimental measurements. Empirical measurements of atmospheric color perception and effects of pollutants over the next few years should provide an adequate means of handling atmospheric discoloration, even without a comprehensive theoretical treatment.

2.3 OPTICAL EFFECTS OF THE ATMOSPHERE AND ITS CONTAINMENTS

2.3.1 Scattering and Absorption

Visibility impairment is caused by the following interactions in the atmosphere:

1. Light scattering -by molecules of air
 -By particles (atmospheric aerosols)
2. Light absorption-by gases
 -By particles

Light scattering by gaseous molecules of air (Rayleigh scattering), which cause the blue color of the sky, is dominant when the air is relatively free of aerosols and light absorbing gases. Light scattering by particles is the most important cause of degraded visual air quality. Fine solid or liquid particles, also known as atmospheric aerosols, account for most of atmospheric light scattering. The aerosols with diameters similar to the wavelength of light (0.1 to 1.0 micrometers) are the most efficient light scatterers per unit mass. Light absorption by gases is particularly important in the discussion of anthropogenic visibility impairment because nitrogen dioxide, a major constituent of power plant and urban plumes, absorbs light. Nitrogen dioxide appears yellow to reddish brown because it strongly absorbs short wavelengths light (blue), leaving longer wavelengths (red) to reach the eye. Light absorption by particles is most important when black soot (finely divided carbon) or large amounts of windblown dust are present. Most atmospheric particles are not, however, generally considered to be efficient light absorbers.

2.3.2 Radiative Transfer

The effect of the intervening atmosphere on the visual properties of distant objects (e.g. the horizon sky, a mountain) theoretically can be determined if the concentration and characteristics of air molecules, aerosols, and nitrogen dioxide are known along the line of sight. The rigorous treatment of visibility requires a mathematical description of the wavelength-dependent interaction of light with the atmosphere, known as the radiative transfer equation. The description presented here is intended to provide a qualitative understanding of this process. Detailed and summary treatments are available in a number of publications. (Chandraskhar, 1950, Latimer et. al., 1978).

Figure 2-9 (a) shows the simple case of a beam of light (e.g. the sun or a searchlight) transmitted horizontally through the atmosphere. The intensity of the beam in the direction of the observer ($I(x)$) decreases with distance from the source as light is absorbed or scattered out of the beam. Over a short interval, this decrease is proportional to the length of the interval and the intensity of the beam at that point.

$$-dI = b_{\text{ext}}I dx \quad (2-1)$$

Where $-dI$ = decrease in intensity (extinction)

b_{ext} = extinction coefficient

I = original intensity of beam

dx = length of short interval

The coefficient of proportionality, denoted by b_{ext} , is called the extinction or attenuation coefficient. The extinction coefficient is determined by the scattering and absorption of particles and gases and varies with pollutant concentration and wavelength of light.

Consider now an observer looking at a distant target, as shown in Figure 2-9b. Just as a beam is attenuated by the atmosphere, the light from the target that reaches the observer

is also diminished by absorption and scattering. The reduced brightness of distant objects is, however, not usually the primary factor limiting their visibility; if it were, the stars would be visible around the clock, since their light must traverse the same atmosphere night and day. In addition to light originating at the target, the observer receives extraneous light scattered into the line of sight by the intervening atmosphere. It is this air light that forms the diaphanous, visible screen we recognize as haze.

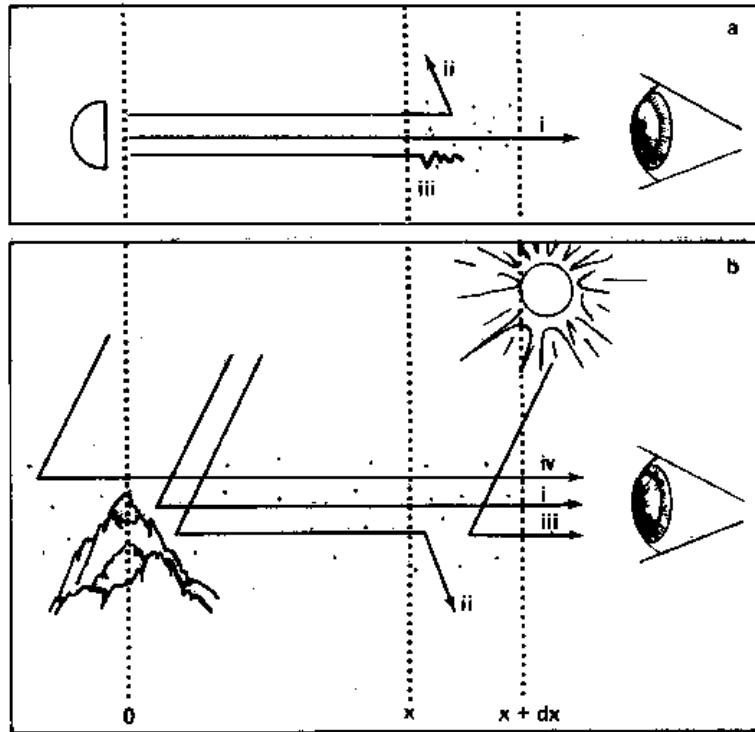


Figure 2-9. (a) A schematic representation of atmospheric extinction, illustrating: (i) transmitted, (ii) scattered, and (iii) absorbed light. (b) A schematic representation of daytime visibility, illustrating: (i) residual light from target reaching observer, (ii) light from target scattered out of observer's line of sight, (iii) airlight from intervening atmosphere, and (iv) airlight constituting horizon sky. (For simplicity, "diffuse" illumination from sky and surface is not shown.) The extinction of transmitted light attenuates the "signal" from the target at the same time as the scattering of airlight is increasing the background "noise."

The intensity of the air light scattered into the sight path of the observer in Figure 2-9b depends on the distribution of light intensity from all directions, including direct sunlight, diffuse sky light or surface reflection, and the light scattering characteristics of the air molecule and aerosols. Over a short interval, the air light added is given by:

$$dI = b_{\text{ext}} \left[W \int Q_v(\theta_v) I_{(v)} d\Omega \right] dx \quad (2-2)$$

Where dI = the increase in intensity from added air light
 b_{ext} = the extinction coefficient

Bracketed parameters [] = the sum of light intensity from all directions scattered into the line of sight. This depends on aerosol and air scattering parameters ($W \Sigma Q_v$), and illumination intensity and angle (I_v, θ_v) summed over all directions (Ω).
 dx = length of short interval

Since both extinction coefficient and other scattering parameters vary with wavelength, the added light can produce a color change.

The overall change in light intensity from an object to an observer is governed by the extinction of transmitted light and the addition of air light. The change in intensity for a short interval (dI) is thus:

$$dI = -dI (\text{extinction}) + dI (\text{air light}) = -b_{\text{ext}} [I dx + W \int Q_v(\theta_v) I_v d\Omega dx] \quad (2-3)$$

This equation, the radiative transfer equation, forms the basis for determining the effects of air pollution on visibility. Its general solution is quite difficult; most visibility models (see Chapter 5) incorporate a number of approximations to simplify calculations and data requirements.

2.3.3. Contrast and Visual Range

The effect of extinction and added air light on the perceived brightness of visual targets is shown graphically in Figure 2-10. At increasing distances, both bright and dark targets are “washed out” and approach the brightness of the horizon. Thus, the apparent contrast of an object relative to the horizon (and other objects) decreases.

An initial object contrast (C_o) can be defined as the ratio of object brightness minus horizon brightness divided by horizon brightness. Assuming a relatively uniform distribution of pollutants and horizontal viewing distance, the apparent contrast of large objects decreases with increasing observer-object distance. As given by Middleton, 1952:

$$C = C_o (B_T b_{\text{ext}} x / B_o) \quad (2-4)$$

Where C = apparent contrast at observer distance

C_o = initial contrast at object

B_T/B_o = ratio of sky brightness at target object to that at observer (usually 1 for distance less than 50-100 km).

b_{ext} = extinction coefficient

x = observer-object distance

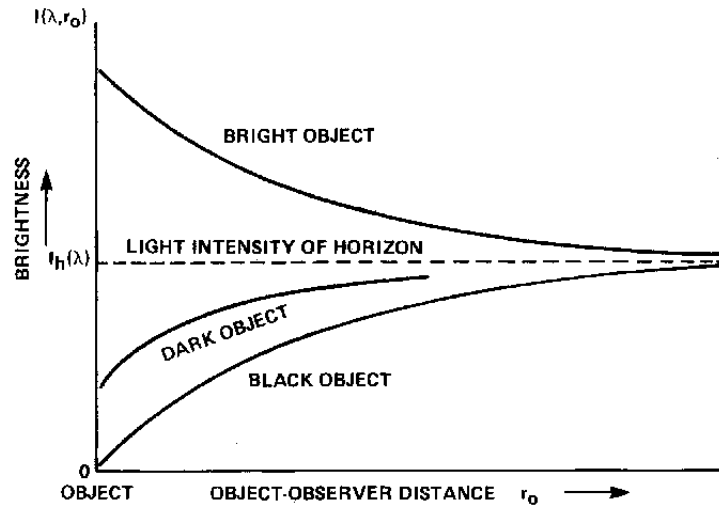


Figure 2-10. Effect of an atmosphere on the perceived brightness of target objects. The apparent contrast between object and horizon sky decreases with increasing distance from the target. This is true for both bright and dark objects (Charlson et al., 1978).

For a black object, the initial contrast is -1 and:

$$C = (-1) e^{-b_{\text{ext}} x}$$

As discussed in the preceding section, the threshold of contrast perception for large dark targets varies between .01 and .05; for “standard” observers a .02 threshold is often assumed (Malm, 1979). In this case, the distance V_r , at which a large black object is just visible is given by:

$$.02 = -e^{-b_{\text{ext}} V_r} \quad \text{or} \quad V_r = 3.92 / b_{\text{ext}} \quad (2-5)$$

This is the standard formula for calculating visual range, originally formulated by Koschmieder in 1924.

The Koschmieder relationship gives a valid approximation of visual range only under a limited set of conditions. Important assumptions and limits are listed and discussed below (Charlson, et. al., 1978, Malm, 1979a):

1. Sky brightness at the observer is similar to the sky brightness at object observed;
2. Homogeneous distribution of pollutants;
3. Horizontal viewing distance;
4. Earth curvatures can be ignored;
5. Large black objects; and
6. Threshold contrast of 0.02.

Assumption 1: The effect on visual range of inhomogeneous illumination, such as that under scattered clouds, is difficult to analyze by elementary methods. Limited experimental evidence indicates that this effect may not be great for short visual ranges (less than 50 km). Visual range has been found to correlate with the reciprocal of the

scattering coefficient, b_{scat}^* , as illustrated in Figure 2-11. The correlation coefficients are commonly in the neighborhood of 0.9, with values for b_{scat} times V_r in the range 2 to 4 as compared to 3.9 in the Koschmieder equation. The studies were conducted in relatively polluted conditions. The effect of scattered clouds or differing sky brightness on visual range in clean areas should be further investigated.

Assumption 2: The Koschmieder equation can be utilized in a non-homogeneous atmosphere (e.g., a ground level plume) if the extinction coefficient in and outside the plume is known. Otherwise, measurements of b_{ext} in areas with strong pollution gradients will produce inaccurate visual range estimates.

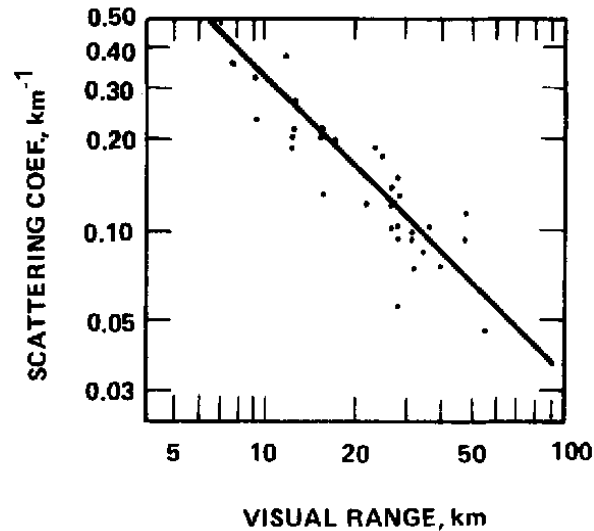


Figure 2-11. Inverse proportionality between visual range and light scattering coefficient (b_{scat}) measured at the point of observation. The straight line shows the Koschmieder formula for non-absorbing ($b_{\text{ext}} = b_{\text{scat}}$) media, $V = 3.9/b_{\text{scat}}$. The linear correlation coefficient for V and b_{scat} is 0.89 (Horvath and Noll, 1969).

Assumptions 3 & 4: Requirements for horizontal viewing distance and curvature of the earth limit the validity of the Koschmieder calculation to cases where visual range is less than about 150-200 km (Figure 2-12). Where no proper targets exist and the extinction coefficient is measured, however, the calculation of visual range is useful in expressing visual air quality in units (miles or kilometers) more readily comprehended by the layman.

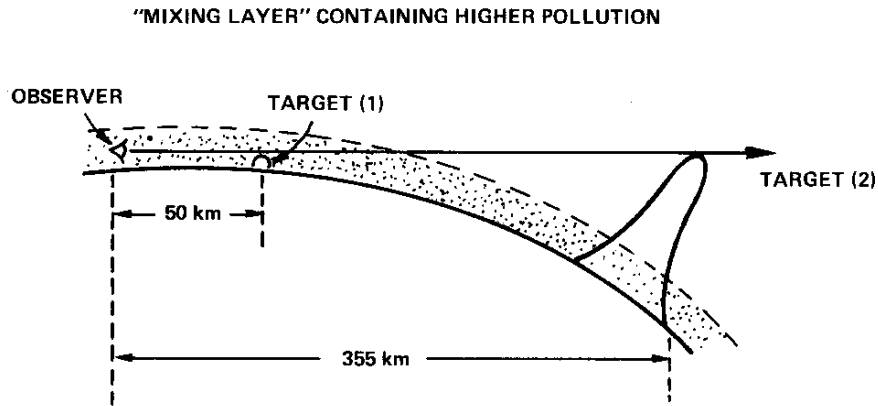


Figure 2-12a. Limitations of Koschmieder relationship. When visual range is short (1), extinction and illumination through sight path is uniform. When true visual range is high (2), Koschmieder equation underestimates visual range because extinction decreases with altitude and illumination (sun angle) at target is different from that at observer. (Dimensions and earth curvature exaggerated for clarity) (Malm, 1979a).

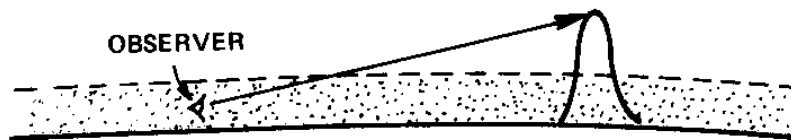


Figure 2-12b. Similarly, when viewing angle is not horizontal, extinction through the sight path is nonuniform. Koschmieder equation will underestimate visual range (Malm, 1979a).

Assumption 5: The visual range for nonblack objects depends strongly on initial contrast, which in turn depends on amount and angle of illumination, or if at night depends on the power of the light source. As a result of this ambiguity, visual ranges for nonblack objects or for lights at night cannot be related simply to each other or to optical air quality.

Assumption 6: The effects of target size, texture, and sensitivity of observer are related to the nature of human perception. As discussed in Section 2.1, in general the "visual range" for small targets or contrast detail is significantly less than that for large objects (Table 2-1).

Detail of objects	Angular size (minutes)	Characteristics sizes at 10 km (m)	Examples for a hillside at 10 km	Visual range (km)	
				West Vr = 100 km	East Vr = 20 km ^b
Very coarse (Form)	> 30'	> 100	Hills, valleys, ridgelines	79-100	16-20
Coarse (Line)	17-30'	50-100	Cliffs faces smaller valleys	76	15
Medium (Texture)	9-17'	25-50	Clumps of large vegetation, clearings on forested slopes	62	12
Fine (Texture)	< 9'	< 25	Individual large trees, clumps of small vegetation	22	4

Table 2-1. Visual Range of Contrast Detail^a. ^aBased on calculations using MTF model of eye-brain response and mathematical transformation of scenic features into a spatial frequency (Henry, 1979). ^bVR sit he assumed background visual range (for large black targets).

2.4 POLLUTANTS THAT IMPAIR VISIBILITY

As indicated above, the air pollution related alteration of the appearance of distant objects (reduction in apparent contrast and visual range) could be estimated if the extinction coefficient, b_{ext} , is known. To the extent b_{ext} varies with the wavelength of visible light, this alteration of appearance includes changes in the apparent coloration of distant objects.

The extinction coefficient represents a summation of the air and pollutant scattering and absorption interactions outlined in 2.3.1.

$$b_{ext} = b_{Rg} + b_{ag} + b_{scat} + b_{ap}$$

Where b_{Rg} is Rayleigh scattering by air molecules;

b_{ag} is absorption by NO₂ gas;

b_{scat} is scattering by particles;

b_{ap} is absorption by particles;

Each of these quantities has inherently different wavelength or color dependence, as will be discussed below. The units of extinction are inverse distance, e.g., 1/mile. The

most commonly used units are km^{-1} and (10^{-4}m^{-1}) . As extinction increases, visibility decreases.

2.4.1 Rayleigh Scatter b_{Rg}

The particle-free molecular atmosphere at sea level has an extinction coefficient of about 0.012 inverse kilometers (km^{-1}) for “green” light (wavelength 0.5 μm), limiting visual range to about 320 km. b_{Rg} decreases with air density and altitude. In some western class I areas, the optical extinction of the atmosphere is at times essentially that of the particle-free atmosphere (Charlson, 1978). Rayleigh scatter thus amounts to a simply definable and measurable background level of extinction against which other extinction components (such as those caused by man-made pollutants) can be compared. Rayleigh scattering decreases with the fourth power of wavelength (Figure 2-13) and contributes a strongly wavelength-dependent component to extinction. When Rayleigh scattering dominates, dark objects viewed at distances of over several kilometers appear behind a blue haze of scattered light, and bright objects on the horizon (such as snow, clouds, or the sun) appear reddened at distances greater than about 30 km.

2.4.2 Absorption by Nitrogen Dioxide Gas (b_{ag})

Of all gaseous air pollutants, only nitrogen dioxide (NO_2) possesses a significant absorption band in the visible part of the spectrum. Nitrogen dioxide and its precursor, nitric oxide (NO), are emitted by high temperature processes such as combustion in fossil-fuel power plants. Nitrogen dioxide is strongly blue absorbing and can color plumes red, brown, or yellow (see Figure 1-6). The hue and intensity of color depend on concentration, optical path length, aerosol properties, conditions of illumination, and observer parameters. In non-urban settings, the area-wide concentration of NO_2 is less important than the levels in coherent plumes. In Figure 2-13, the absorption of 0.1 ppm NO_2 , a concentration found in urban areas, is compared to the spectral extinction of pure air. At a wavelength of 0.55 μm , the absorption by NO_2 is comparable to air scattering. The absorption coefficient drops off rapidly with wavelengths, which can give a brownish color when viewed against a white background. However, at concentrations more typical of class I areas, (less than 0.01 ppm) area-wide impacts of NO_2 absorption are unimportant.

2.4.3 Particle Scattering (b_{scat}) and Absorption (b_{ap})

As the particle concentration increases from very low levels where Rayleigh scatter dominates, the particle scattering coefficient b_{scat} increases until eventually $b_{\text{scat}} > b_{\text{Rg}}$. At this point, particle scattering controls the visual quality of air. In understanding the degradation of visual quality of air two principal problems have been:

1. Defining the size range and other physical characteristics of particles most effective in causing scatter and
2. Defining the chemical composition and, thus, identifying the source of particles in this optically effective size range (Charlson et al., 1978).

2.4.3.1 Light Scattering and Absorption by Single Particles—Particle size, refractive index, and shape are the most important parameters in relating particle concentration and

particle derived extinction coefficients, b_{scat} and b_{ap} . If these properties are established, the light scattering and absorption can be calculated. Alternatively, the extinction coefficient associated with an aerosol can be measured directly (see Chapter 3).

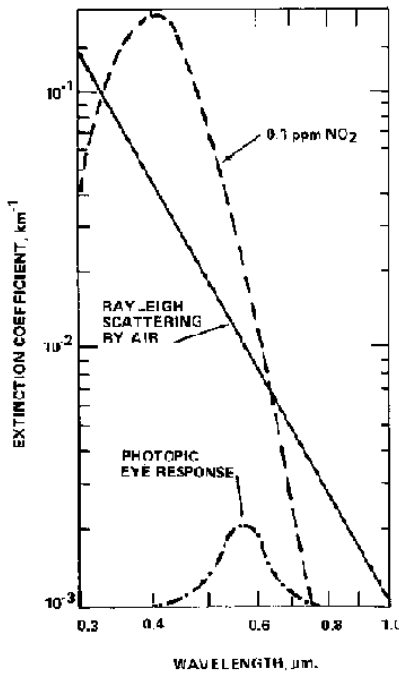


Figure 2-13. Rayleigh scattering by air (b_{Rg}) is proportional to (wavelength)⁴. Reduced air density at higher altitudes causes a reduction of b_{Rg} . The NO_2 absorption band peaks at $0.4 \mu\text{m}$ but vanishes in the red portion of the spectrum (Husar et al., 1979).

The basic interactions between light and atmospheric particles are illustrated in Figure 2-14. For spherical particles of sizes similar to the wavelength of visible light (0.1 to $1 \mu\text{m}$), the scattering and absorption of individual particles can be calculated through use of the “Mie” equations (Mie, 1908).

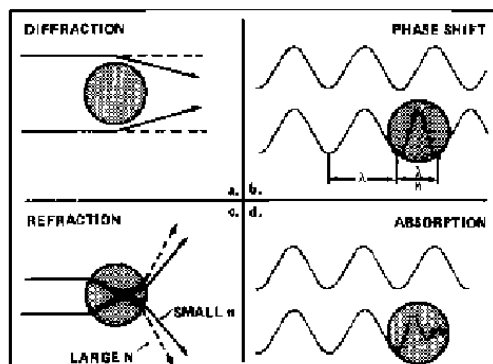


Figure 2-14. Light scattering by coarse particles ($>2\mu\text{m}$) is the combined effect of diffraction and refraction. A) Diffraction is an edge effect whereby the radiation is bent to “fill the shadow” behind the particle. B) The speed of a wavefront entering a particle with refractive index $n > 1$ (for water $n = 1.33$) is reduced. This leads to a

reduction of the wavelength within the particle. Consequently a phase shift develops between the wave within and outside the particle leading to positive and negative interferences. C) Refraction also produces the "lens effect." The angular dispersion by bending of incoming rays increases with n . D) For absorbing media, the refracted wave intensity decays within the particle. When the particle size is comparable to the wavelength of light (0.1 - 1 μm), these interactions (a-d) are complex and enhanced. For particles of this size and larger, most of the light is scattered in the forward hemisphere, or away from the light source.

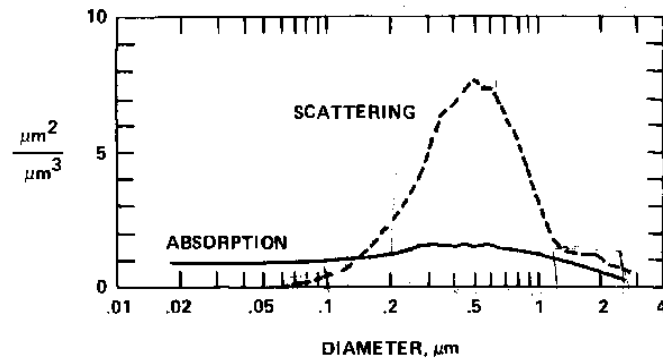


Figure 2-15. Single Particle Scattering and Absorption. For a single particle of typical composition the scattering per volume has a strong peak at particle diameter of 0.5 μm ($m = 1.5 - 0.051$; wavelength: 0.55 μm). The absorption per aerosol volume however is only weakly dependent on particle size. Thus the light extinction by particles with diameter less than 0.1 μm is primarily due to absorption (Charlson et al. 1978). Scattering for such particles is very low. A black plume of soot from an oil burner is a practical example.

Charlson et al., (1978) used Mie theory to calculate the light scattering and absorption efficiency per unit volume of particle for a typical aerosol containing some light absorbing soot (Figure 2-15). As illustrated in the figure, particles in the size range of 0.1 to 1 μm are the most efficient light scatterers. The remarkably high scattering efficiencies of these particles are illustrated by the following examples: a given mass of aerosol of 0.5 μm diameter scatters about a billion times that of the same mass of air; a 1 mm thick sheet of transparent material, if dispersed as 0.5 μm particles, is sufficient to scatter 99% of the incident light, i.e. to obscure completely vision across such aerosol cloud (Husar et. al., 1979).

Atmospheric particles or aerosols are made up of a number of chemical compounds. All of these compounds exhibit a peak scattering efficiency in the same particle size range as that calculated for the typical aerosol of Figure 2-15. Because of differences in refractive index, however, the values of the peak efficiency and the particle size at which it occurs vary considerably among the compounds.

From Figure 2-16 it is apparent that, for relating light scattering to the aerosol, consideration needs to be given to the chemical composition of the scattering and absorbing aerosol. In particular, compounds that tend to draw water in the aerosol phase, such as sulfates, can be very important. Furthermore, the optical properties of a given

mass of aerosol collected over the arid western part of the country may be substantially different from those of the same mass of aerosol collected in a humid eastern U.S. air mass.

2.4.3.2 Characteristics of Atmospheric Particles—Investigations of atmospheric aerosols over the past several years have revealed some important regular features (Whitby et al., 1972). A typical atmospheric particle size distribution is shown in Figure 2-17. Most of the aerosol volume and mass is distributed in two modes: a fine mode centered at about $0.3 \mu\text{m}$ and a coarse mode centered at 5 to $30 \mu\text{m}$. The two modes are usually unrelated in that they have different compositions, sources, life times, and removal mechanisms. Figure 2-18 illustrates a pair of measured particle size distributions showing independent variation of fine particle concentration at a single site.

The source of much of the fine mode particles is atmospheric transformation of reactive gases (e.g. sulfur dioxide, volatile organics, and ammonia) into aerosols such as sulfates, particulate organics, and ammonium compounds. Such transformed substances are called *secondary* particles. Other important fine mode sources include direct or *primary* particle emissions from combustion (fires, automobiles, etc.) and industrial processes. Coarse mode particles usually are derived from mechanical processes such as grinding operations or plowing. High winds can suspend large quantities of coarse particles.

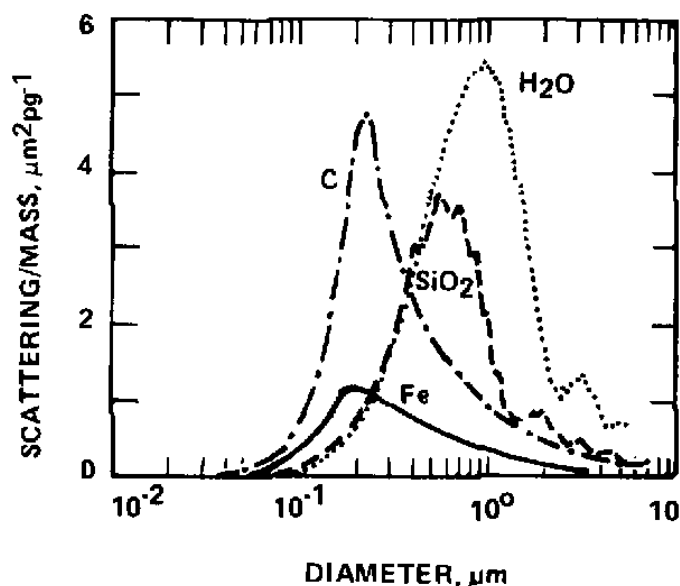


Figure 2-16. Single particle light scattering for several substances. Per unit mass, water scatters more light than SiO_2 or iron. Furthermore, the water scattering efficiency peaks at about $1 \mu\text{m}$, while the spheres of pure carbon or iron are most efficient scatterers at $0.2 \mu\text{m}$ (Faxvog, 1975). Carbon is the most efficient light absorbing substance, and hence $0.2 \mu\text{m}$ carbon particles are the most efficient for total extinction (absorption + scatter) (Faxvog and Roessler, 1978).

From the point of view of aerosol optics, a key question is whether an aerosol particle is spherical. For such particles, rigorous Mie theory is applicable and the optical properties can be readily calculated from their size and reflective index. Measurements

in St. Louis by Allen et al(1978) show that in the fine mode less than 5% of aerosol population exhibits nonspherical shape. Puschel and Wellman (1978) found that spherical particles also dominate fine mode aerosols near Cedar Mountain, Utah. Coarse particles are almost exclusively nonspherical and therefore the application of the Mie theory to calculate their optical properties is only a crude approximation. Currently there is an extensive body of experimental data on the optical properties of the nonspherical particles (e.g. Pinnick et al., 1976).

2.4.3.3 Light Scattering by Typical Particle Distributions—Measured particle size distributions can be used in conjunction with Mie theory calculations for single particles as shown in Figures 2-15 and 2-16, to determine the contribution of different size classes to extinction. The result of this kind of calculation is shown in Figure 2-19. The peak in single particle scattering per unit volume at 0.3 μm coincides with the peak in observed aerosol volume (mass), so that the fine particles dominate extinction in most cases.

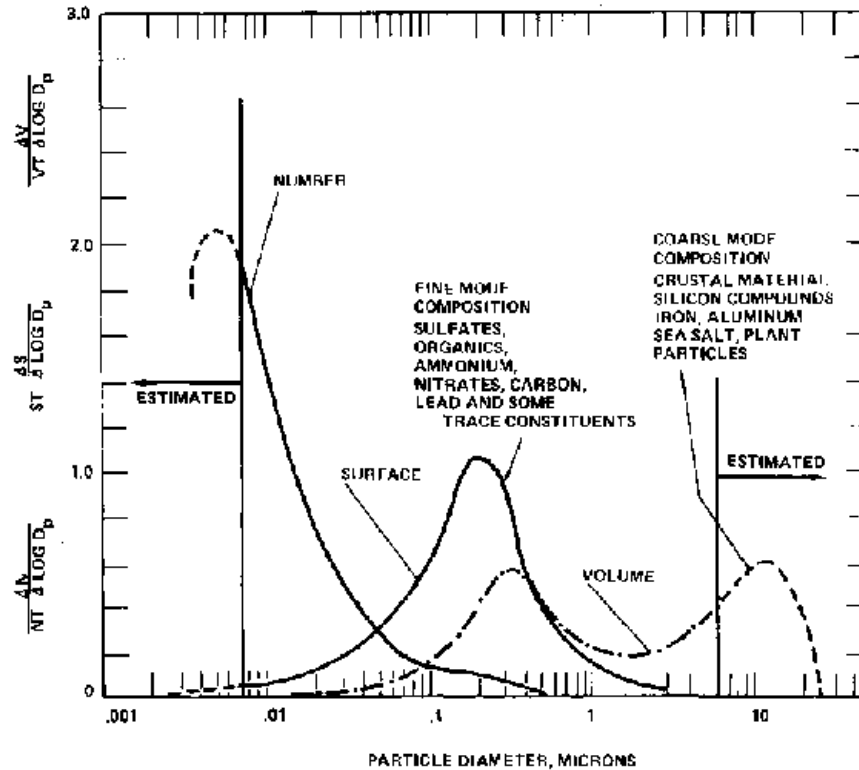


Figure 2-17. Number, Surface, and Volume (Mass) distributions for typical aerosols in the lower atmosphere. Their typical chemical constituents of each mode are also given. The area under each curve segment is proportional to the fraction of the property (number, N; surface, S; volume, V) that is contained within a given size range (Whitby et al., 1972).

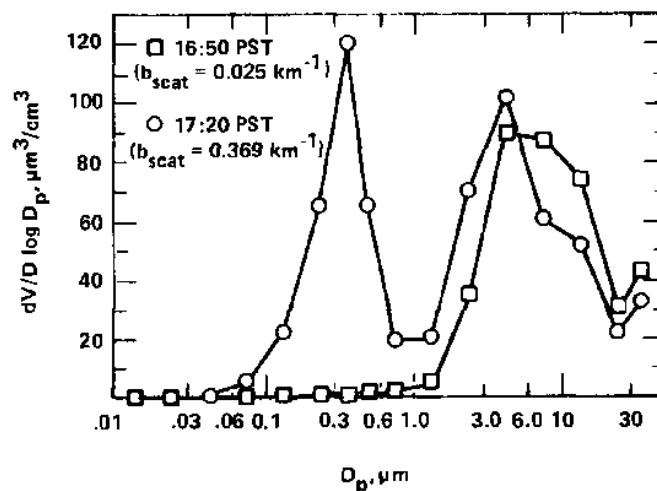


Figure 2-18. Variation in Fine and Coarse Particle Modes. In the California ACHEX study, the measured aerosol distributions have shown that the fine and coarse particle modes are essentially independent. In Rubidoux, for example, the size distribution has been observed to change from a fine particle-free distribution at 16:50 (Sept. 25, 1973) to the usual bimodal distribution at 17:20 (Hidy et al., 1975).

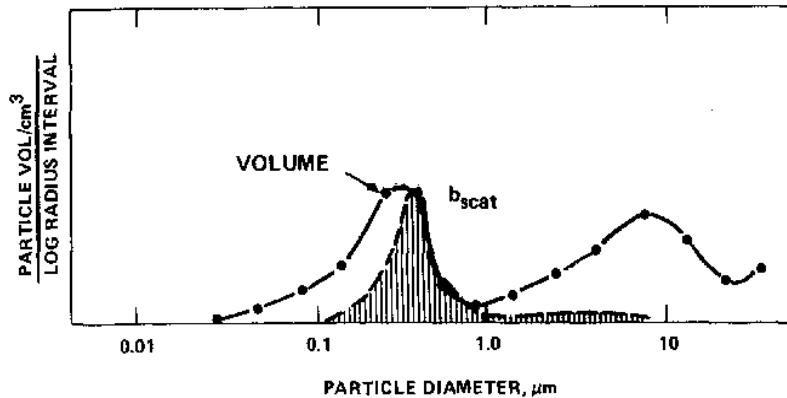


Figure 2-19. Light scattering for a typical aerosol volume (mass) distribution. The calculated light scattering coefficient is contributed almost entirely by the size range 0.1 - 1.0 μm . The total b_{scat} and total aerosol volume are proportional to the area under the respective curves (Charlson et al., 1978).

Because the peak and shape of the bimodal particle mass distribution curve can vary, the light scattering characteristics of a given particle mass might also be expected to vary. As noted by Charlson (1978), however for the observed range of atmospheric particle distributions, the calculated scattering coefficient per unit mass is relatively uniform. Latimer et al. (1978) have determined the scattering efficiency per unit mass for several aerosol distributions. The calculated coefficient changes by no more than 40 percent in the size range of 0.2 to 1.0 μm (Figure 2-20).

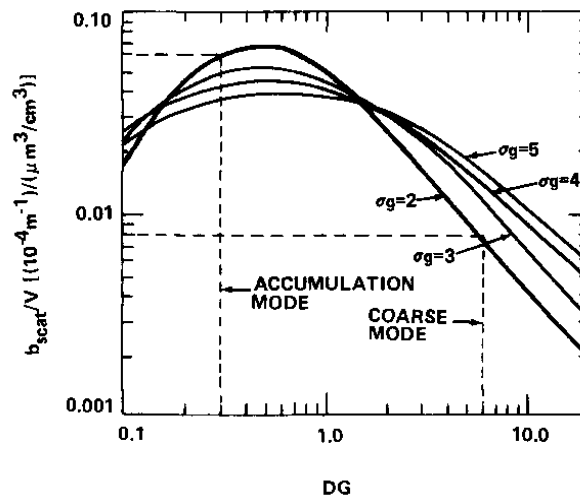


Figure 2-20. The light scattering per unit volume for various aerosol size distributions (σ_g) is the highest in the 0.2 - 1.0 μm range, and does not vary greatly (Latimer et al., 1978).

The relative consistency of calculated light scattering per unit mass over a range of particle distributions and the dominant influence of fine particles suggest that reasonably good approximations of light scattering coefficients can be obtained by measurements of fine particle mass. Simultaneous monitoring of the two parameters at a number of sites has been conducted by several investigators (Weiss, 1978, Patterson and

Wagman, 1978, Macias et al., 1975, and White and Roberts, 1975). These investigators measured scattering per unit mass ratios of $0.003 \text{ km}^{-1}/\mu\text{g}/\text{m}^3$ to $0.005 \text{ km}^{-1}/\mu\text{g}/\text{m}^3$ at several locations. The Mie calculations of Figure 2-19 suggest a ratio of $0.0033 \text{ km}^{-1}/\mu\text{g}/\text{m}^3$. Moreover, at these locations, correlations between fine particle mass and b_{scat} were consistently 0.95 or better. Figure 2-21 shows the relationship for St. Louis. The high correlations indicate that at the sites studied, fine particle mass dominates particle scattering. The relationship between several chemical components of fine particles and light scattering is discussed in Chapter 4.

Coarse particles are a less significant cause of visibility degradation. Notable exceptions include wind-blown dust, fog, fly ash, and certain plumes. In case of wind-blown dust, for example, Gillette et al. (1978) have reported light scattering to mass ratios more than an order of magnitude lower than the ratios noted above, since coarse dust particles are much less efficient scatterers per unit mass (Figure 2-15). In clean areas where fine particle levels are low, however, coarse mode particle may contribute a non-negligible portion of light scattering. Secondly, it should be noted that a given b_{scat} to mass ratio is only applicable if the refractive indexes of the light scattering particles are the same. It is conceivable that, in the dry and arid western states, the aerosol refractive index and relative amounts of coarse and fine mode particles are sufficiently different that the scattering mass ratios quoted above would not be applicable. Preliminary results from project VISTTA, however (Macias, et al., 1979) suggest b_{scat} /fine mass ratios in the southwest are $0.003 \text{ km}^{-1}/\mu\text{g}/\text{m}^3$, or about the same as measured elsewhere.

The wavelength dependence of light scattering ranges from the very strong blue scattering of air molecules and very small particles $<0.05 \mu\text{m}$ to wavelength independent to “white” scattering for coarse particles $> 5 \mu\text{m}$. Thus Rayleigh particles ($<0.05\mu\text{m}$) in the exhaust of a poorly tuned automobile appear blue against a dark background while a fog of coarse water droplets appears white. A typical aerosol size distribution at moderate concentrations tends to scatter more blue light than red, but the wavelength dependence is not as strong as for Rayleigh particles. It has generally been observed that the wavelength dependence of light scattering diminishes as the total light scattering and humidity increases (Husar et al., 1979).

In pristine class I areas on days when Rayleigh scattering dominates ($b_{\text{Rg}} = 0.012 \text{ km}^{-1}$), an addition of about $4 \mu\text{g}/\text{m}^3$ of fine particles ($b_{\text{scat}} = 0.013 \text{ km}^{-1}$) would cause substantial “whitening” of the natural blue Rayleigh haze and the horizon sky (Charlson et al., 1978). At a fine particle level of $30 \mu\text{m}/\text{m}^3$ (0.1 km^{-1}), the wavelength dependent scatter would be controlled by the aerosol itself.

2.4.3.4 Light Absorption by Typical Particle Distributions—Particle absorption (b_{ap}) appears to be on the order of 10 percent of particle scattering (b_{scat}) in clean background areas (Bryce Canyon, Utah) and up to 50 percent of composition and particle size distribution (Waggoner, 1973, Bergstrom, 1973). The most important contributor to this absorption (in cities) appears to be graphitic carbon in the form of soot (Novakov et al., 1978). The source of this highly absorbing submicrometer soot appears to be the combustion of liquid fuels, particularly in diesel engines; coal combustion may not be a major contributor (Charlson et al., 1978).

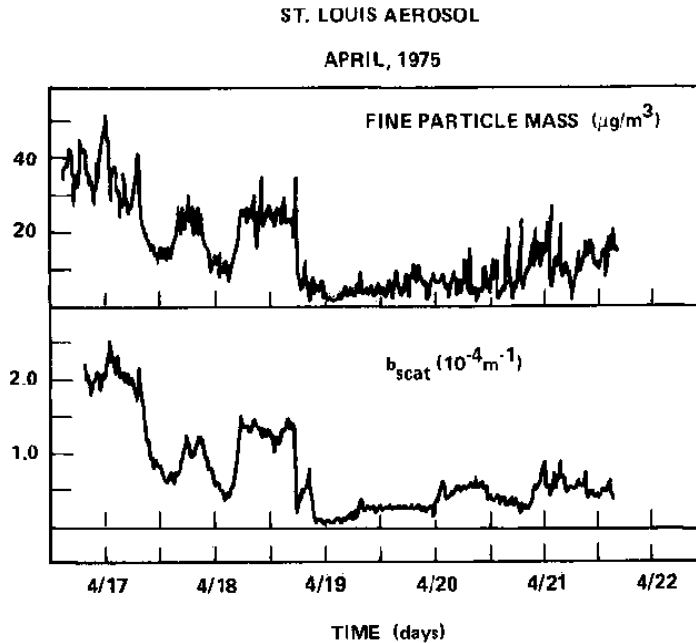


Figure 2-21. Light scattering vs. fine particle mass. Simultaneous monitoring of b_{scat} and fine particle mass in St. Louis showed a high correlation coefficient of 0.96, indicating that b_{scat} depends primarily on the fine particle mass concentration (Macias et al., 1975).

2.5 POLLUTANT/IMPAIRMENT RELATIONSHIPS

The scattering and absorption from an aerosol cloud depend on the wavelength of incident light, the angle of observation, and the concentration and size distribution of the light scattering and absorbing aerosol and gases. The role of these parameters will be examined briefly as applied to the three major types of visibility impairment: general haze, plume blight, and atmospheric discoloration.

2.5.1 General Haze—Visual Range, Contrast, Color

Visibility in the atmosphere of pristine class I areas is extremely sensitive to incremental additions of fine aerosol. The sensitivity of clean atmospheres to change is illustrated in the graph of visual range versus extinction (fine particle mass) in Figure 2-22.

However, in many class I areas, where viewing distances are 50 to 100 km, a reduction in calculated visual range (for example, from 350 km to 250 km) will not be the most noticeable impact of incremental pollution. The reduction in apparent contrast and discoloration of nearby objects and sky are the main effects perceived in such areas.

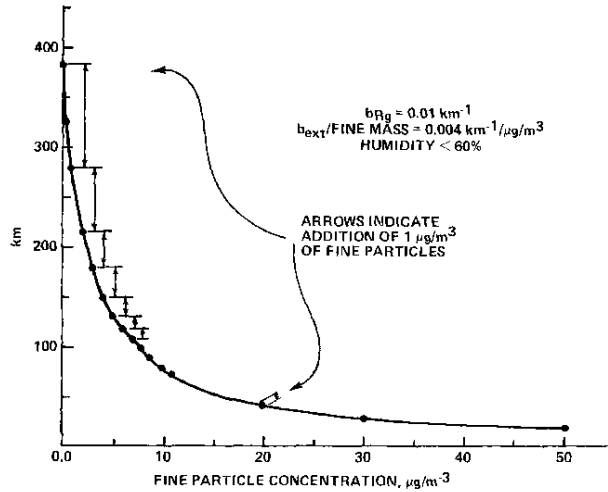


Figure 2-22. Effects of fine particle increments on calculated visual range. Addition of $1 \mu\text{g}/\text{m}^3$ to a clean atmosphere reduces visual range by 30 percent. Addition of the same amount when background visual range is 35 km (20 miles) produces a 3 percent reduction.

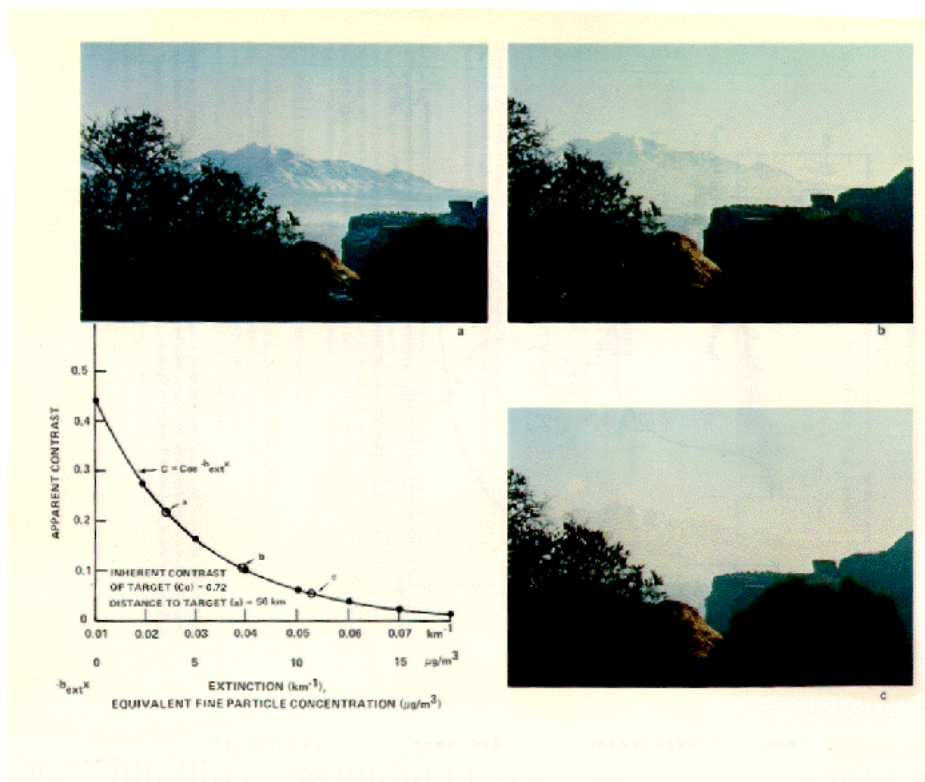


Figure 2-23. Effect of fine particle increments (calculated) on apparent contrast (measured) between sky and target (mountain) (Malm, 1979b).

Figure 2-23 shows that apparent contrast between an object and sky also decreases rapidly with increasing extinction in clean atmospheres. The graph also indicates the calculated concentration of fine particles spread throughout the viewing distance associated with the listed extinction coefficient. The accompanying photographs show the dramatic changes in contrast detail of even a 3 to 5 $\mu\text{g}/\text{m}^3$ increment of fine particles. A similar increment in a relatively polluted area (20 $\mu\text{g}/\text{m}^3$ of fine particles) might not be perceptible. Calculation of contrast changes (for large targets) accompanying incremental particle levels indicate that the maximum decrease in contrast will occur for objects located at distances of about one-fourth of the visual range from the observer (Malm, 1979a). Thus, in an initially clean atmosphere, a fine particle increment produces maximum contrast reduction for large objects 50 to 100 km away. A reduction in visual range of 5 percent would result in a reduction in contrast of 0.02 for those objects. As discussed in Section 2.2.1, such a change may be just perceptible. The contrast detail (texture, small objects) and coloration of closer objects in contrast may, however, be affected to a greater degree (Henry, 1979, Malm, 1979a).

The perceived color of objects and sky is also changed by the addition of aerosols. Because of the difficulties and uncertainties in specifying perceived color, only a qualitative description is possible. In general, the apparent color of any target fades toward that of the horizon sky with increasing distances from the observer. Without particles, scattered air light is blue, and dark objects appear increasingly blue with distance. The addition of small amounts (1 to 5 $\mu\text{g}/\text{m}^3$) of fine particles throughout the viewing distance tends to whiten the horizon sky making distant dark objects and intervening air light (haze) appears grayer. According to Charlson et al., (1978), even though the visual range may be decreased only slightly from the limit imposed by Rayleigh scattering the change from blue to gray is an easily perceived discoloration. The apparent color of white objects is less sensitive to incremental aerosol loadings. As for contrast, incremental aerosol additions produce a much greater color shift in cleaner atmospheres (Malm, 1979a).

Aerosol haze can also degrade the view of the night sky. Light scattering and absorption diminish star brightness. Perception of stars is also reduced by an increase in the brightness of the night sky caused by scattering of available light. In or near urban areas, particle scattering of artificial light significantly increases night sky brightness. The combination of extinction of starlight and increased sky brightness markedly decreases the number of stars visible in the night sky at fine particle concentrations of 10 to 30 $\mu\text{g}/\text{m}^3$ (Leonard et al., 1977).

Thus, the overall impact of aerosol haze is to reduce visual range and contrast, and change color. Visually the objects are “flattened” and the aesthetic value of the vista is degraded even though the distances are small relative to the visual range. Much of the scenic value of a vista can be lost when the visual range is reduced to a distance that is several times greatest line-of-sight range in the scene.

2.5.2 Discolored Layers

Layers of colored haze can be caused by particles and nitrogen dioxide. The visual impact depends greatly on a number of factors such as sun angle, surrounding scenery, sky cover, viewing angle, perception parameters, and pollutant loading. Quantitative

theoretical treatments of these effects, combining radiative transfer and human perception, are not fully developed. The following general observations can, however, be made (Charlson et al., 1978):

1. The relative importance of aerosol or NO_2 in determining the color and appearance of a plume or haze layer can be addressed, in part, in terms of the relative extinction as a function of wavelength.
2. Suspended particles generally scatter much more in the forward direction than in other directions. This fact means a plume or haze layer can appear bright in forward scatter (sun in front of observer) and dark in back scatter (sun in back of observer) because of the angular variation in scattered air light (Figure 2-24). This effect can vary with background sky and objects.
3. The added air light (see 2.3.1) is both angle and wavelength (color) dependent and the wavelength dependence can vary with illumination angle. Extinction is wavelength dependent but not angle dependent.
4. A visible aerosol layer will be brighter than an adjacent particle-free layer for sun angles (in front of observer) less than 30° . At larger angles, the aerosols will usually be darker.
5. Aerosol optical effects alone are theoretically capable of imparting a reddish-brown color to a haze layer when viewed in backward scatter. NO_2 would increase the degree of coloration in such a situation. Specific circumstances of brown layers must be examined on a case-by-case basis.

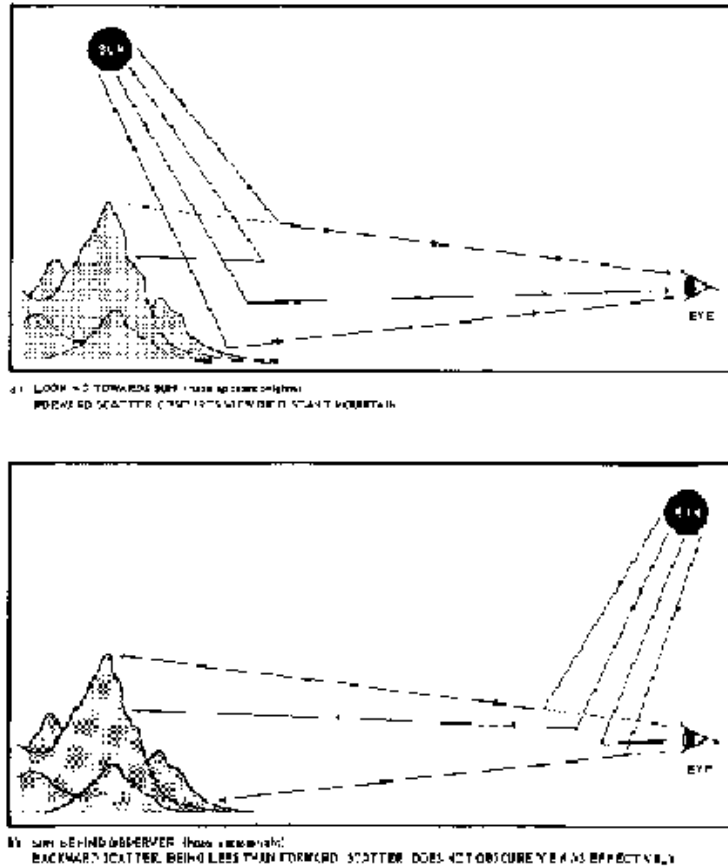


Figure 2-24. Effect of sun angle on visibility.

2.5.3 Plume Blight

The description of discolored layers in the previous section applies to plume blight. The significant factors affecting plume visibility are listed in Table 2-2 and Figure 2-25. The plume will have a brightness and color that is different from its background, and this difference can be approximated by simplifications to the radiative transfer operation for optically “thin” plumes; that is, plumes that transmit a large fraction of incident light (Latimer et al., 1978, Williams et al., 1979).

The plume air light is a strong function of scattering sun angle. A plume viewed in forward scatter will appear bright against the sky or background targets. The same plume can appear dark against the sky and bright against dark targets at scattering angles greater than 30° . Detailed calculation for models requires particle concentration and size information for the plume and similar information or extinction measurements for the surrounding atmosphere. Increases in extinction resulting from plume absorption, from soot or NO_2 , for example, will make the plume darker at all sun angles.

Because the line of demarcation between the plume and sky is “fuzzy,” it has been argued (Latimer et al., 1978) that the threshold contrast for perception may be greater than that for dark targets with sharp boundaries (about 2 percent). Contrast enhancement* by the eye-brain system may, however, compensate for lost sharpness.

Additional experimental data are needed to define the threshold of perceptibility for plumes and haze layers.

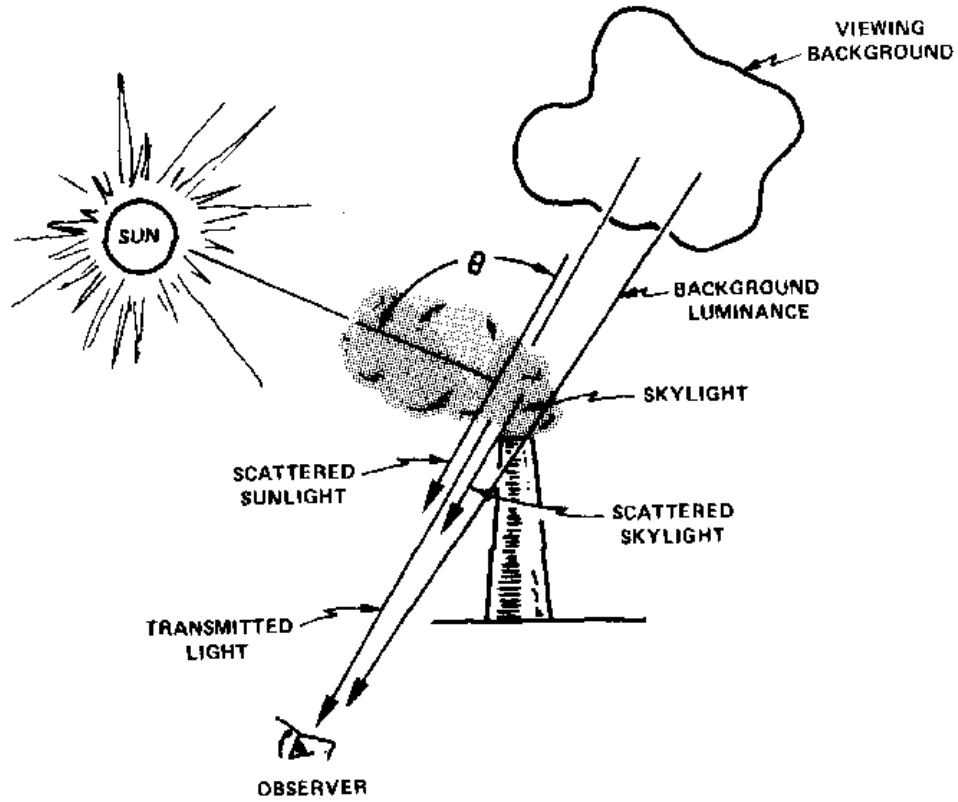


Figure 2-25. Appearance of a plume (Charlson et al., 1978).

<u>Plume/source related factors</u>	<u>Environmental Factors</u>
Particle size distribution	Sun position
Particle mass concentration	Time of day
Particle mass distribution (non-uniform mass distribution)	Day of year
Plume diameter	Longitude
Stack height	Latitude
Stack exit velocity	Cloud cover (sky color)
Particle density	Other light sources
Water vapor content	Ambient temperature
Particle complex index of refraction (plume color)	Relative humidity
NO ₂ concentration in the plume	Wind velocity
	Wind direction
<u>Observer related factors</u>	Wind turbulence
Observer position	Terrain
Observer sensitivity	Background

Table 2-2. Factors affecting plume appearance (Charlson et al., 1978).

REFERENCES FOR CHAPTER 2

Allen, J., R. B. Husar, and E. S. Macias (1978) In: *Aerosol Measurement*, Lundgren, D.A. Ed., University of Florida Press, Gainesville, Fla.

Bergstrom, R. W. (1973) Extinction and Absorption Coefficients of the Atmospheric Aerosol as a Function of Particle Size. *Beitr A. Phys. Atm.*, 46: 223. *Beitr A. Phys. Atm.*, 46: 223.

Blackwell, H. R. (1946) Contrast Thresholds of the Human Eye. *J. Opt. Soc. Amer.* 36: 642-643. Brown, W. R. S. (1957) Color Discrimination of Twelve Observers. *J. Opt. Soc. Amer.* 47: 142.

Campbell, F. W., and L. Maffei (1974) Contrast and Spatial frequency. *Scientific American* 231: 106-112. Chandrasekhar, S. (1950) *Radiative Transfer*, Clarendon, Oxford.

Charlson, R. J., A. P. Waggoner, and J. F. Thielke, (1978) Visibility Protection for Class I Areas. The Technical Basis. Report to Council of Environmental Quality. Washington, D.C.

Faxvog, F. R. (1975) Optical Scattering per Unit Mass of Single Particles. *Applied Opt.* 14: 269-270. Faxvog, F. R. , and Roessler (1978) Carbon Aerosol Visibility versus Particle Size Distribution. *Applied Opt.* 17: 261-262.

Gillette, D. A., R. N. Clayton, T. K. Mayeda, M. L. Jackson, K. Sridhar, (1978) Tropospheric Aerosols From Some Major Dust Storms of the Southwestern U.S. *Journal of Applied Meteorology* 17: 832-845.

Gregory, R. L. (1978) *Eye and Brain: the Psychology of Seeing*. McGraw-Hill Book Co., New York.

Henry, R. C. (1977) The Application of the Linear System Theory of Visual Acuity to Visibility Reduction by Aerosols. *Atmospheric Environment* 11: 697-701.

Henry (1979) Psychophysics and Visibility Values. In: *Proceedings of the Workshop on Visibility Values*, Fox, D. , R. J. Loomis and T. C. Greene (Technical Coordinators). Fort Collins, Colorado. U .S. Department of Agriculture.

Hidy, G. M. et al. (1975) *Characterization of Aerosols in California*. Report SC 534.25 FR 4. California Air Resources Board, Contract 358, Rockwell Science Center, Thousand Oaks, California.

Horvath, H. (1971) On the Applicability of the Koschmieder Visibility Formula. *Atmospheric Environment* 5: 177-184.

Horvath, H., and K. E. Noll, (1969) The Relationship Between Atmospheric Light Scattering Coefficient and Visibility. *Atmospheric Environment* 3: 543-550.

Husar, R., W. H. White, D. E. Patterson, and J. Trijonis (1979) Visibility Impairment in the Atmosphere, Draft report prepared for U.S. Environmental Protection Agency under Contract Number 68022515, Task Order No.28.

Konig, A., and E. Brodhum (1889) Experimentelle Untersuchungen ueber die physchaphysische Fundamen- talformel in Bezug auf den Gesichtssinn.

Land, E. H. (1977) The Retinex Theory of Color Vision, *Scientific American*, 108-128, December.

Latimer, D. A., R. W. Bergstrom, S. R. Hayes, M. K. Liu, J. H. Seinfeld, G. Z. Whitten, M. A. Wojcik, M. J. Hillyer, (1978) The Development of Mathematical Models for the Prediction of Anthropogenic Visibility Impair- ment, EPA-450/3/78-110a.

Leonard, E. M., M. D. Williams, and J. P. Mutschlecner, (1977) The Visibility Issue in the Rocky Mountain West, Prepared by Los Alamos Scientific Laboratory for the Department of Energy , preliminary draft report, September 30.

MacAdam, D. D. (1942) Visual Sensitivities to Color Differences in Daylight. *J. Opt. Soc. Amer.* 32: 247-273.

Macias, E. S., R. B. Husar, J. D. Husar, (1975) Monitoring of Atmospheric Aerosol Mass and Sulfur Concentration. International Conference on Environ. Sensing and Assessment. Las Vegas, Nevada, September.

Macias, E. S., D. C. Blumenthal, J. A. Anderson, B. K. Cantrell, (1979) Characterization of Visibility, Reducing Aerosols in the Southwestern United States; Interim Report on Project VISTT A MRI Report 78 IR 15-85.

Malm W. (1979a) Visibility: A Physical Perspective. In: Proceedings of the Workshop in Visibility Values, Fox, D., R. J. Loomis and T. C. Greene (technical Coordinators). Fort Collins, Colorado, U.S. Dept. of Agriculture. p. 56-68

Malm, W. (1979b) Personal Communication, Environmental Protection Agency, Environmental Monitoring and Support Laboratory, Las Vegas, Nevada.

Middleton, W. E. K. (1952) *Vision through the Atmosphere*, University of Toronto Press, Toronto, Canada.

Mie. G. (1908), Beitrage zur optic truber Medien, speciell kolloidaler Metallosungen. *Ann. Phy.* 25: 377.

Niemann, B. L., E. Y. Tong, M. T. Mills and L. Smith (1979) Characterization of Regional Episodes of Particulate Sulfates and Ozone over the Eastern United States and Canada. Paper to be presented at Symposium on Long-Range Transport, World Meteorological Organization, Sofia, Bulgaria, October, 1979.

Novakov, R., et al. (1977) Report, LBL-6819, Lawrence-Berkley Laboratory, Berkeley, California.

Patterson, D. K. and J. Wagman, (1977) Mass and Composition of an Urban Aerosol as a Function of Size for Several Visibility Levels. *J. Aerosol Sci.* 8: 262-279.

Pinnick, R. G., D. E. Carroll, and D. J. Hofmann, (1976) Polarized light scattered from Monodispersal Randomly Oriented Non-spherical Aerosol particle measurements *Appl. Optics* 15: 384.

Pueschel, R. F., and D. L. Wellman (1978) On the Nature of the Atmospheric Background Aerosol. Atmospheric Physics and Chemistry Laboratory, National Oceanic and Atmospheric Administration, Boulder, Colorado.

Taylor, J. H. (1964) Practice Effects in a Simple Visual Detection Task. *Nature*, 201: 691.
Waggoner, A.P., et al. (1973) Optical Absorption by Atmosphere Aerosols. *Applied Optics* 12:896.
Weiss, R. (1978) P.h.D. Dissertation, University of Washington, Seattle, Washington.

Whitby, K. T., R. B. Lussar, and Lui, B.Y.H. (1972) The Aerosol Size Distribution, *J. Colloid Interface Sci.*, 39: 177-204.

White, W. H., and P. T. Roberts, (1975) On the Nature and Origins of Visibility-Reducing Aerosols in the Los Angeles Air Basin, W. M. Keck Laboratories, California Institute of Technology.

Williams, M. D., E. Treiman, M. Weeksung (1979) Utilization of a Simulated Photograph Technique as a Tool for the Study of Visibility Impairment LA-UR-79-1741, Los Alamos Scientific Laboratory, Los Alamos, N.M.